On proximity correction of pipe-type cable parameters with method of moment approach

H. K. Høidalen, M. Høyer-Hansen, F. N. Camara, C. L. Bak

Abstract **– Cable parameters are used to establish models of cables for transient and steady-state analysis. Finite element methods (FEM) can calculate such parameters accurately but are time consuming and demanding, thus not always suitable in an engineering process. In contrast, classical analytical equations for parameter calculations are simple and fast but do not properly take proximity effects into account. This is particularly important in cables with common screens but also in complicated umbilical cables and pipe cases. This paper briefly reviews the MoM-SO method for series impedance and shunt admittance. This is then applied as extensions to classical pipe-type cable parameters procedures. Two cases demonstrate the accuracy of the proposed method when compared to FEM analysis. A simple three-core cable case shows very good agreement, while a special pipe-in-pipe geometry reveals some challenges. The required order of the method increases with the radius ratio of the conductors involved. A final simulation case shows that analytical methods for pipe-type cables underestimates damping but have little effect on the wave velocity.**

Keywords**: Cable parameters, proximity effect, capacitance, series impedance.1**

I. Introduction

Cable parameters are critical for adequate analysis of the power system. These parameters can be calculated numerically by finite element methods (FEM), but this slows down the engineering process considerable. Establishing a model in FEM can easily take hours and days, while the engineering demand today is minutes and seconds. Thus, cable parameters calculated by most electromagnetic program are based on the analytical formulas efficiently summarized by Ametani [1]. These formulas do not take proximity effect properly into account, although for pipe-type cables this is partially addressed. The analytical method of moment with a surface operator (MoM-SO) was presented by Patel et.al. in [2, 3]. In this work, the geometry of circular elements and periodic current contribution were represented by an analytical Green's function, and each conductor by an admittance representing the frequency dependency with surface currents. Later, Tanaka et.a. [4,5] presented capacitance correction based on the same Greens function.

In this paper we first for motivation present two test cases where the analytical calculated cable parameters significantly deviate from what is calculated by FEM, in Section II. Then we briefly outline the MoM-SO method for the basic understanding of the method's complications in Section III. Further we discuss the integration in EMTP type of software and present new calculation result in agreement with FEM in Section IV. Finally, we discuss the result in Section V and conclude with main findings and proposed further work in Section VI.

II. Analytical formulation vs. FEM

Here we present two cases with significant deviations between analytical cable parameters and FEM. The analytical formulas for calculating the series impedance and shunt capacitance are given in [1] both for single core and pipe-type cables. Here we focus on the pipe-internal impedance and potential coefficients.

According to [1] the potential coefficient of a pipe type cable is $P=P_i+P_p+P_c+P_o$ where P_i represents each cable, P_p is the potential between cables inside the pipe, P_c comes from the pipe's outer insulation and P_o is zero when the pipe is in ground. In our further analysis the P_i and P_o components are zero. The pipe internal and external coefficients are

$$P_{pi,i} = \frac{Q_{i,i}}{2\pi\varepsilon_r\varepsilon_0},\quad P_{pi,j} = \frac{Q_{i,j}}{2\pi\varepsilon_r\varepsilon_0} \quad \text{and} \quad P_c = \frac{\ln(r_{p3}/r_{p2})}{2\pi\varepsilon_r\varepsilon_0} \tag{1}$$

$$\text{with}\quad Q_{i,i} = \ln\left(\frac{r_{p1}}{r_i}\left(1-\left(\frac{d_i}{r_{p1}}\right)^2\right)\right) \quad \text{and} \tag{2}$$

$$\begin{aligned} Q_{i,j} &= \ln\left(\frac{r_{p1}}{\sqrt{d_i^2+d_j^2-z}}\right) - \sum_{n=1}^{\infty}\frac{C_n}{n} \\ &= \ln\sqrt{\frac{r_{p1}^2+(d_i d_j/r_{p1})^2-z}{d_i^2+d_j^2-z}} \end{aligned} \tag{3}$$

$$\text{with}\; z = 2d_i d_j\cos(\theta_{ij}) \quad \text{and} \quad C_n = \left(\frac{d_i d_j}{r_{p1}^2}\right)^n \cdot \cos\left(n\theta_{ij}\right) \tag{4}$$

where the geometrical parameters are given in Fig. 1. According to [1] the series impedance of a pipe type cable is $Z=Z_i+Z_p+Z_c+Z_o$ where Z_i represents each cable, Z_p is the impedance between cables inside the pipe, Z_c comes from the impedance of the pipes itself, and Z_o is the ground return impedance. In our further analysis the Z_i and Z_p components are subjected to proximity effect. Here we restrict the analysis to the mutual impedances of cables inside a pipe, Z_p.

$$Z_{pi,j} = \frac{j\omega\mu_0}{2\pi}\left[\frac{\mu_{rp}K_0(x_1)}{K_1(x_1)} + Q_{i,j} + Q_\Sigma\right] \tag{5}$$

H. K. Høidalen is with the Department of Electric Power Engineering, Norwegian University of Technology (NTNU), Trondheim.
(e-mail: hans.hoidalen@ntnu.no). M. Høyer-Hansen is with SINTEF, Norway, F. N. Camara is with DNV, Norway and C. L. Bak is with Aalborg University, Denmark.

Paper submitted to the International Conference on Power Systems Transients (IPST2025) in Guadalajara, Mexico, June 8-12, 2025.

where $Q_\Sigma = 2\mu_{rp} \cdot \sum_{n=1}^{\infty} \frac{C_n}{n(1+\mu_{rp}) + x_1 \cdot K_{n-1}(x_1)/K_n(x_1)}$ (6)

$x_1 = r_{p1} \cdot \sqrt{j\omega\mu_p\sigma_p}$, K is second modified Bessel function.

A. Power cable, case 1

The first case is a (low-voltage) screen less cable design as shown in Fig. 1. Here the problem is the screenless design and the short insulation distances. The permittivity of the entire insulation medium inside the pipe is assumed to have the same permittivity.

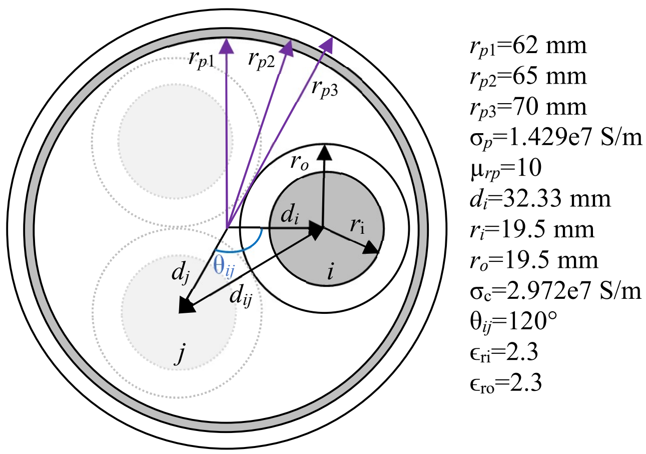

Fig. 1 Geometry of pipe-type cable design 1.

Fig. 2 shows a FEM simulation in COMSOL of the cable design in Fig. 1. It is rotated -30 degrees, but this does not matter in this symmetrical design. 1 A is applied to the right conductor with return in the pipe. We see that the induced currents in the two neighbor conductors show sign of proximity effect, while the current in the excited conductor looks fairly symmetrical.

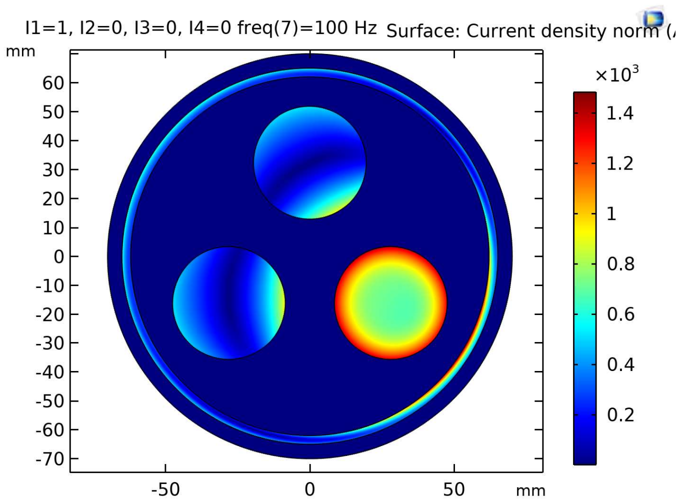

Fig. 2 FEM simulation. Current density at 100 Hz.

Fig. 3 shows and compares the calculated series impedance Z_i+Z_p self- and mutual impedance from COMSOL and CABLE PARAMETERS in ATP-EMTP that uses the analytical formulas. The contribution from the pipe impedance, Z_c and the ground return Z_o is eliminated by subtracting the last column and row. Fig. 3 shows that the reactance is somewhat larger by the analytical formulations, while the resistance is underestimated. The deviations are larger for the mutual impedance Z_{12}.

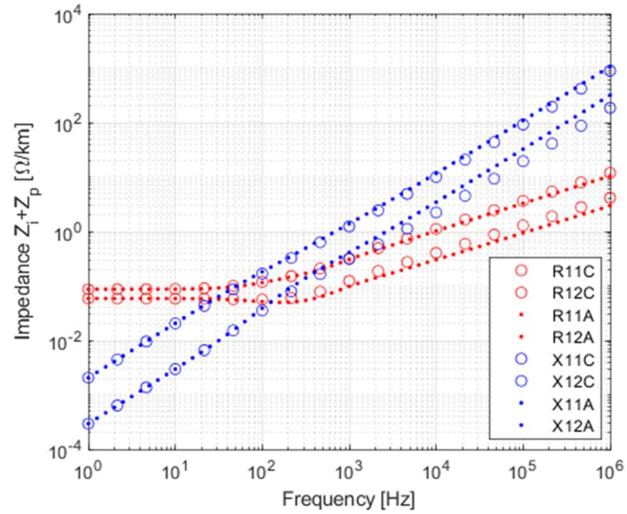

Fig. 3 Comparison of series impedance. Reactance in blue and resistance in red colors. COMSOL calculations marked as circles, analytical formulas with dots. R_{11} and X_{11} are larger than R_{12} and X_{12}, respectively.

The 4x4 cable capacitance matrix of the configuration in Fig. 1 is calculated in COMSOL and MatLab and shown in Table I. We observe considerable differences even for this simple design. The analytical formula is developed from the impedance formula at infinite frequency [6].

TABLE I. COMPARISON OF CAPACITANCE VALUES, CASE 1.

C [nF/km]	1	2	3	4
COMSOL	196.41	-33.53	-33.53	-129.35
ANALYT	176.65	-40.58	-40.58	-95.49
COMSOL	-33.53	196.41	-33.53	-129.35
ANALYT	-40.58	176.65	-40.58	-95.49
COMSOL	-33.53	-33.53	196.41	-129.35
ANALYT	-40.58	-40.58	176.65	-95.49
COMSOL	-129.35	-129.35	-129.35	2114.6
ANALYT	-95.49	-95.49	-95.49	2013.1

B. Pipe-in-pipe heating cable, case 2

The second example if from an oil&gas pipe-in-pipe installation where small heating cables are installed close to a large internal pipe as shown in Fig. 4. Here the problem is the large difference in dimensions and the short distance between the conductors. The purpose of analysis in such system is primarily fault studies and corrosion prevention. The capacitances to ground are very relevant for analyzing these heating systems, often performed with isolated neutral.

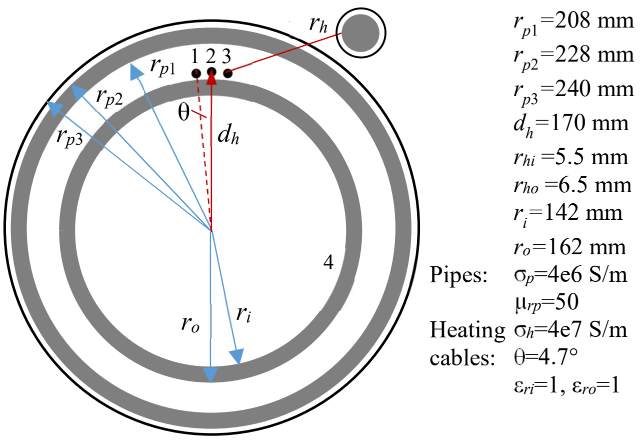

Fig. 4 Geometry of pipe-type cable Case 2 consisting of two steel pipes. Heating cables are installed close to inner pipe and shown zoomed up outside

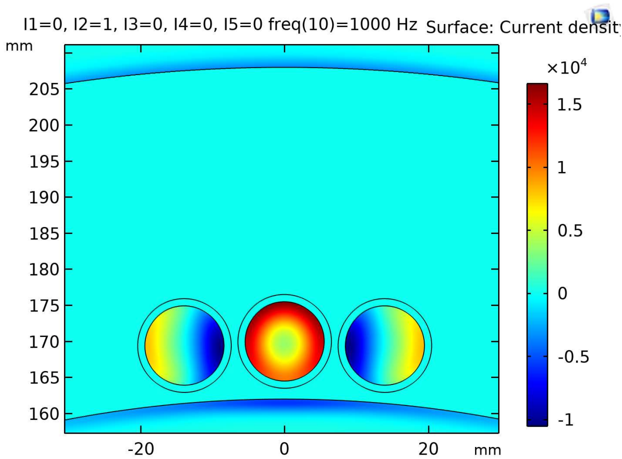

Fig. 5 FEM simulation. Current density at 1 kHz. 1 A applied to the middle heating conductor with return in the outer pipe.

Fig. 6 shows the calculated series impedance Z11 and Z12 with COMSOL and CABLE PARAMETERS in ATP-EMTP. We see that the reactance is considerably overestimated in the analytical formulas at high frequency, while the resistance is underestimated.

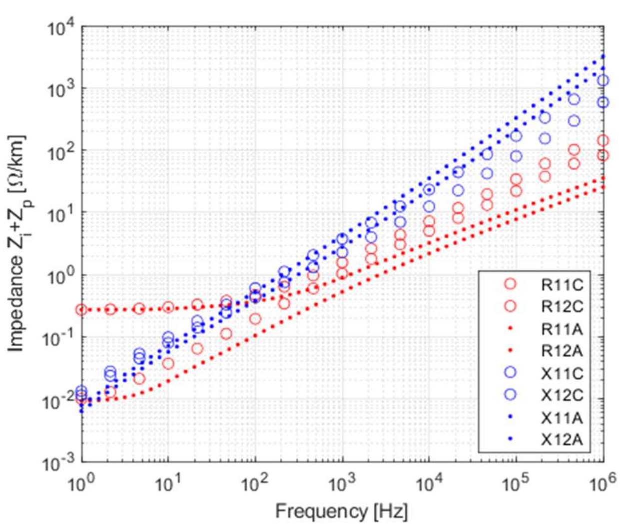

Fig. 6 Comparison of series impedance. Reactance in blue and resistance in red colors. COMSOL calculations marked as circles, analytical formulas with dots. R_{11} and X_{11} are larger than R_{12} and X_{12}, respectively.

We now calculate the capacitances in the system in Fig. 4 both analytically in MatLab and numerically in COMSOL as shown in Tabl. II. We set the outer pipe insulation to zero to reduce the system to 4x4. We identify huge differences between the values and the capacitance between the two outer heating cables (1-3, separation angle 9.4°) becomes even negative by the analytical formulas.

TABLE II. COMPARISON OF CAPACITANCE VALUES, CASE 2

C [nF/km]	1	2	3	4
COMSOL	75.809	-25.074	-0.5573	-43.689
ANALYT	37.939	-24.571	+1.978	-12.387
COMSOL	-25.074	89.884	-25.074	-35.367
ANALYT	-24.571	53.749	-24.571	-3.794
COMSOL	-0.5573	-25.074	75.809	-43.689
ANALYT	+1.978	-24.571	37.939	-12.387
COMSOL	-43.689	-35.367	-43.689	332.88
ANALYT	-12.387	-3.794	-12.387	245.58

III. IMPLEMENTATION OF THE METHOD-OF-MOMENT

The MoM-SO method for proximity correction of circular conductor is described in detail in [2, 3] and only the elements relevant for the implementation for pipe-type cables will be outlined here. A contribution is simplifications of the formulas.

A. Basic expressions

The method is an analytical boundary element approach that consists of an expanded Greens function (G) taking a space periodic surface current into account, and a Surface admittance Operator (Y_S). The boundary element surface current is assumed to be written as a Fourier series with a maximum order N_p.

The series impedance is in [2, 3] defined as

$$Z = \left[U^T \cdot \left(1 - j\omega\mu_0 Y_S \cdot G\right)^{-1} Y_S \cdot U\right]^{-1} \tag{7}$$

The shunt capacitance is similarly defined in [4] as

$$C = -\varepsilon \cdot V^T \cdot G^{-1} \cdot V \tag{8}$$

where U, V are connection matrices containing 1s or 0s linking the fundamental element to the external conductor.

The Greens function is established for each conductor and between each conductors including the pipe. Its elements for conductors outside each other are defined in [2] and repeated in in (9) for the self-elements (p=q) and in (10) for the mutual element (p≠q):

$$G^{p,q}_{n',n} = \frac{1}{2\pi}\begin{cases} \ln(r_p), n = n' = 0 \\ \dfrac{-1}{2|n|}, n' = n \neq 0 \end{cases} \tag{9}$$

$$G^{p,q}_{n',n} = \frac{1}{2\pi}\begin{cases} \ln(d_{p,q}), & n' = n = 0 \\ \dfrac{-1}{2|n'|}\left(\dfrac{r_p}{d_{p,q}}\right)^{|n'|} \cdot \left(\dfrac{-x_{p,q} + jy_{p,q}}{d_{p,q}}\right)^{n'}, & n = 0 \\ \dfrac{-1}{2n}\dfrac{r_q^n}{(-r_d)^{n'}}\begin{pmatrix} n-n'-1 \\ -n' \end{pmatrix} \cdot \left(x_{p,q} - jy_{p,q}\right)^{-n+n'}, & n > 0, n' < 1 \end{cases} \tag{10}$$

If the conductor p is inside q we have

$$G_{n',n}^{p,q} = \frac{1}{2\pi}\begin{cases} \ln(r_q), & n' = n = 0 \\ \dfrac{-r_p^{n'}}{2n \cdot r_q^{n}}\dbinom{n}{n'}\cdot\left(x_{p,q} + jy_{p,q}\right)^{n-n'}, & n' \geq 0,\ n' \leq n \end{cases} \tag{11}$$

and for q inside p similarly

$$G_{n',n}^{p,q} = \frac{1}{2\pi}\begin{cases} \ln(r_p), & n' = n = 0 \\ \dfrac{-r_q^{n}}{2n' \cdot r_p^{n'}}\dbinom{n'}{n}\cdot\left(-x_{p,q} + jy_{p,q}\right)^{n'-n}, & n \geq 0,\ n \leq n' \end{cases} \tag{12}$$

where (:) are binomial coefficients.

There are symmetries involving complex conjugates applied for $n<0$ $G_{n',n}^{p,q} = \left(G_{-n',-n}^{p,q}\right)^{*}$. (13)

For each tubular conductor, there will be two equivalent conductors as explained in [3].

The surface admittance operator is in [2, 3] given as

$$Y_{s,n}(\omega) = \frac{2\pi}{j\omega\mu_0}\left(\frac{1}{\mu_r}\cdot R(|n|,k) - R(|n|,k_0)\right) \tag{14}$$

where $k = \sqrt{\omega\mu(\omega\varepsilon - j\sigma)}$ and $k_0 = \omega\sqrt{\mu_0\varepsilon_0}$ are the wave numbers in the conductor or free space respectively, and n is the order.

For a solid conductor R is a scalar quantity [2]:

$$R(n,k) = -n + k\cdot r\cdot\frac{J_{n-1}(k\cdot r)}{J_n(k\cdot r)} \tag{15}$$

and for tubular conductors (r_o, r_i are outer and inner radiuses) R is a 2x2 matrix on the form (simplified from [3]):

$$R_{1,1}(n,k) = -n + \frac{N_n(k\cdot r_o, k\cdot r_i)}{D_n(k\cdot r_o, k\cdot r_i)}$$

$$R_{2,2}(n,k) = -n + \frac{N_n(k\cdot r_i, k\cdot r_o)}{D_n(k\cdot r_o, k\cdot r_i)} \tag{16}$$

$$R_{1,2}(n,k) = \frac{2}{\pi}\frac{1}{D_n(k\cdot r_o, k\cdot r_i)} = R_{2,1}(n,k)$$

where

$$N_n(\alpha,\beta) = \beta\cdot\left[J_n(\alpha)\cdot Y_{n+1}(\beta) - J_{n+1}(\beta)\cdot Y_n(\alpha)\right] \text{ and}$$

$$D_n(\alpha,\beta) = J_n(\alpha)\cdot Y_n(\beta) - J_n(\beta)\cdot Y_n(\alpha) \tag{17}$$

J and Y are Bessel functions of the first and second kind, respectively.

B. Structure of MoM-SO matrices

Two conductors inside a pipe are shown in Fig. 7. A solid conductor is called conductor 1, a tubular conductor with inner and outer surfaces called conductors 2 and 3, and the pipe that becomes conductors 4 and 5. Fig. 8 and 9 shows the structure of the G and Y_s matrices respectively for this geometry.

For the capacitance calculation in (8), all conductors can be set as solid. There will thus only be three conductors in Figs. 8 and 9 and the structure will be as the first 3x3 sub-matrices.

Eq. (7) and (8) will produce series impedance and capacitance with size 3x3 for the configuration in Fig. 7.

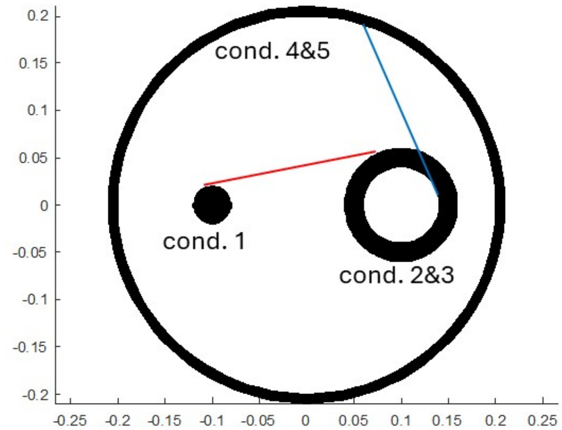

Fig. 7 Generalized configuration of conductors used in MoM-SO.

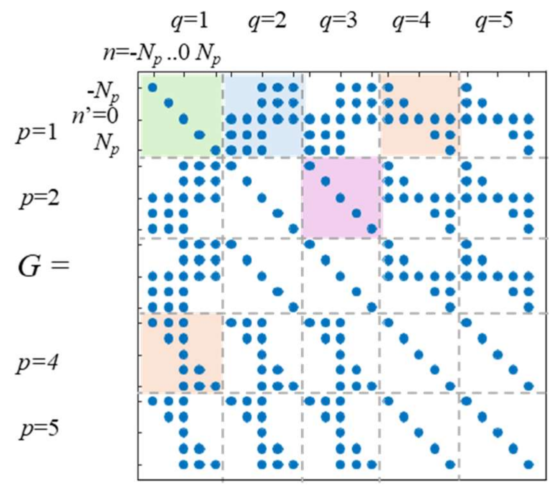

Fig. 8 Structure of the Greens function. Blue dots show non-zero elements of sub-matrices $G_{n',n}^{p,q}$. Green: Self element, blue: outside conductors, orange: conductors inside each other, pink: inside centered conductors.

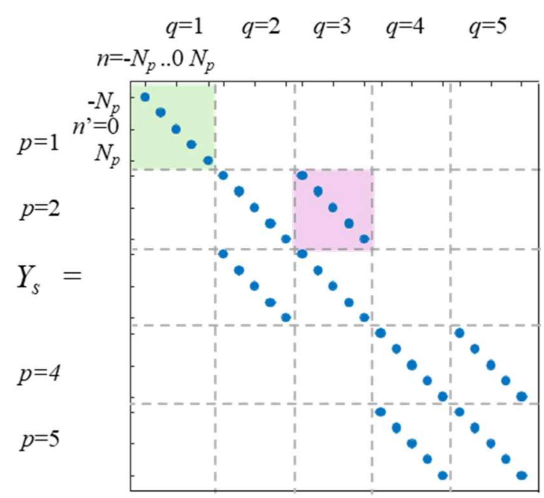

Fig. 9 Structure of the surface admittance matrix. Blue dots show non-zero elements. Colored rectangle shows the structure of sub-matrices $Y_{sn',n}^{p,q}$. Green: Self element, pink: mutual elements ($Y_S^{1,2}$) for tubular conductors.

C. Conditioning and order selection

The functions (15) and (16) are ill-conditioned and must be series expanded at low arguments and asymptotic expanded at large arguments. Unfortunately, no closed form series expansion seems to exist as function of the order n. Thus, separate expansions must be made for each order. This expansion must handle cases where the inner and outer radiuses are close. And for non-magnetic material the contribution from the conductor and free space in (14) cancel each other. These requirements pose a practical limit on the possible order. The large argument asymptotic expansion can be found as a closed form as function of the order n, for example:

$$\lim_{\omega\to\infty} R_{11} = \frac{k\cdot r_i}{\tan(k(r_o-r_i))}+\frac{1}{2}+\frac{(n^2-1/4)(r_o-r_i)}{2r_o\sin^2(k(r_o-r_i))}+\ldots \qquad (18)$$

but even with this expression care must be taken evaluating the complex, trigonometric functions.

D. Implementation in Cable Parameters

With the basis in Cable Parameters [1] we propose a method where the proximity effect correction only applies to the P_p and Z_p pipe internal potential and series impedance expressions in (1) and (5). The purpose is to not alter the calculation of the cable internal potential P_i or impedance Z_i.

First, we calculate the series impedance according to (7) for order N_p and subtract a similar calculation with order N_p =0. In both cases we use the pipe as the reference conductor and eliminate its row and column from the contribution [7]. This gives us the incremental proximity effect contribution in addition to the conductor internal impedance Z_i.

$$Z(N_P) = Z_i + \Delta Z_{prox} \quad \text{and} \qquad (19)$$

$$Z(N_P=0) = Z_i + \frac{j\omega\mu_0}{2\pi}\ln(r_{p1}/r) \qquad (20)$$

Since, Z_p in (5) already contains parts related to proximity effect we must modify (5) by setting C_n=0 (in both (3) and (6)) and further let $Q_{i,i} \to \ln(r_{p1}/r_i)$. This gives us the modified pipe-internal impedance where also the Bessel term is updated for finite pipe thickness as proposed in [8].

$$\begin{aligned} Z_{pi,i} &= \frac{j\omega\mu_0}{2\omega}\cdot\ln(r_{p1}/r_i) + Z_{pi} + Z(N_P) - Z(N_P=0) \\ &= Z_{pi} + \Delta Z_{prox} \end{aligned} \qquad (21)$$

with

$$Z_{pi} = \frac{j\omega\mu_0}{2\pi}\cdot\frac{\mu_{rp}}{x_1}\frac{I_0(x_1)\cdot K_1(x_2)+I_1(x_2)\cdot K_0(x_1)}{I_1(x_2)\cdot K_1(x_1)-I_1(x_1)\cdot K_1(x_2)} \qquad (22)$$

For the potential coefficients P_p we calculate this once for order N_p. The potential contribution from the pipe is based on the outer radius of the conductors and the inner radius of the pipe. This potential P_p is then added to the internal potential from the conductor P_i. The dual insulation media method proposed in [4] is not implanted so far.

IV. Results

Here we show the result of calculation of series impedance and capacitance using the Greens function and surface admittance matrices outlined in Sect. III.

A. Power cable, case 1

The case 1 in Fig. 1 is now recalculated from (21) for the series impedance and from (8) for the capacitance. We see that the parameters now are in agreement with COMSOL using order N_p=4 both for series impedance and capacitance.

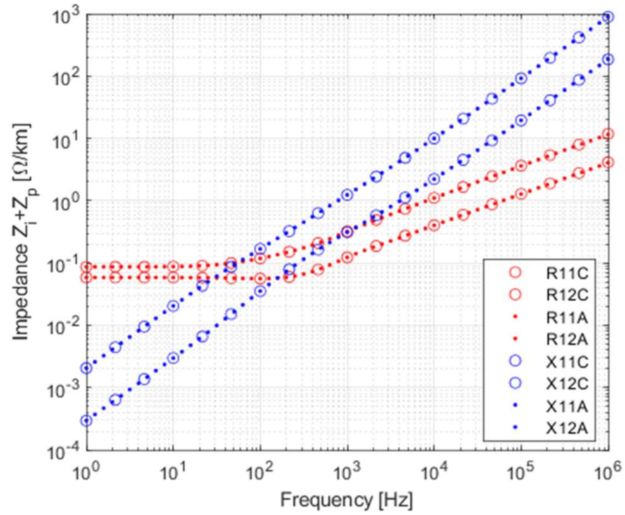

Fig. 10 Comparison of series impedance. Reactance in blue and resistance in red colors. COMSOL calculations marked as circles, MoM-SO with N_p=4 with dots.

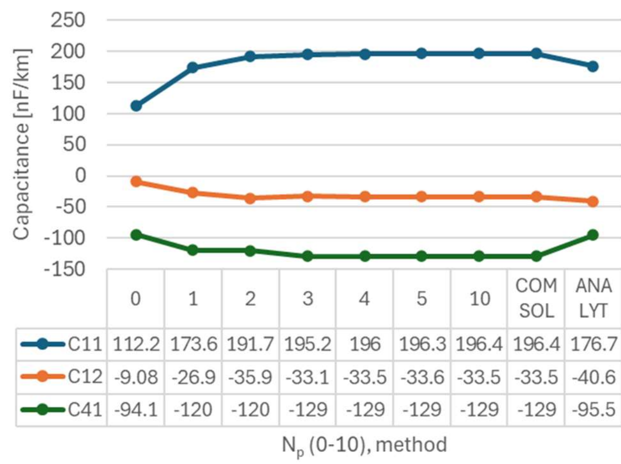

Fig. 11 Calculation of capacitance using MoM method as function of order N_p.

Tabl. III shows the calculation speed per frequency point of the implemented MoM-SO method for Case 1 together with the analytical cable parameter calculation when C_n in (3) and (6) is set to zero or not. The calculation time is dominated by the proximity correction for the series impedance made for every frequency point (91 in this case) while the capacitance correction is calculated once.

TABLE III. CALCULATION TIME CASE I. CPU 3GHZ, INTER CORE I7-9700

Time/Freq [ms]	MoM-SO	Cable Parameters	
		C_n=0	C_n≠0 (3, 6)
N_p=3	2.4	0.15	1.6
N_p=4	4.6	0.15	1.6
N_p=5	7.8	0.15	1.6
N_p=6	12.5	0.15	1.6

B. *Pipe-in-pipe heating cable, case 2*

The case in Fig. 4 is now recalculated from (21) for the series impedance and from (8) for the capacitance. Fig. 12 shows the result with order N_p=6. The agreement is still not sufficient at this order. We have thus repeated the calculation with order N_p=13 in Fig. 13.

The evaluation at order N_p=13 was possible since the low argument expansion of (14)-(15) (supported only up to order N_p =6) was not needed in this case. No further improvement was possible beyond order N_p =13 due to numerical issues with Bessel/Hankel function evaluations.

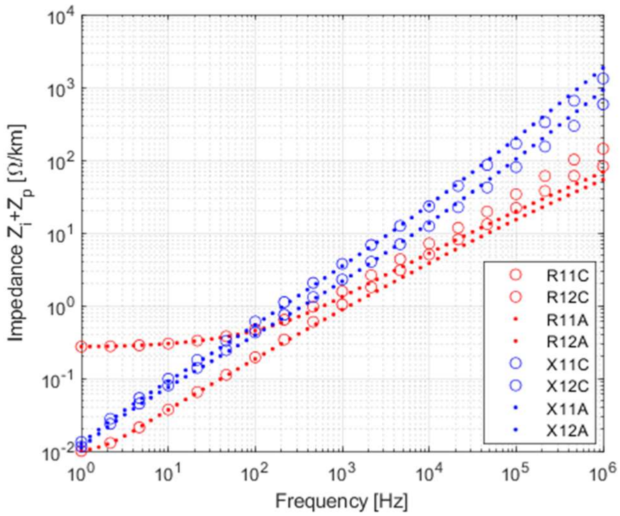

Fig. 12 Comparison of series impedance. Reactance in blue and resistance in red colors. COMSOL calculations marked as circles, MoM-SO with N_p=6 with dots.

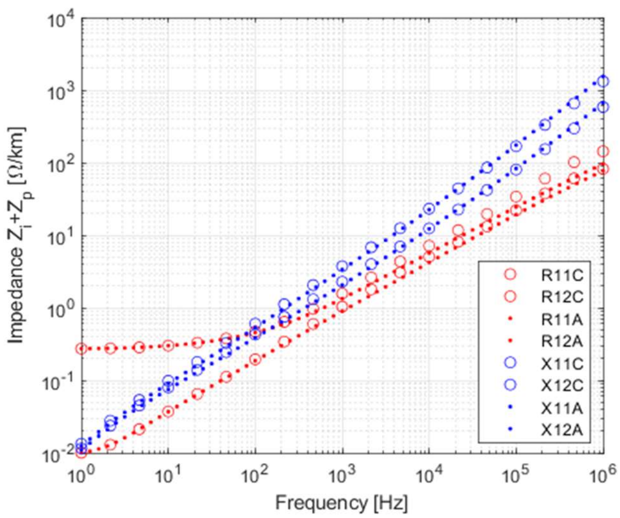

Fig. 13 Comparison of series impedance. Reactance in blue and resistance in red colors. COMSOL calculations marked as circles, MoM-SO with N_p=13 with dots.

Fig. 14 shows how the capacitances are evaluated as function of the order N_p. Orders above 50 is required for the capacitance. Above order N_p=75 numerical issues with inverting the G-matrix appeared. It is important to note that the result in Fig. 14 was obtained only if the outer insulation of the conductors was removed. This is justified only if the permittivities of the conductor insulation and the pipe insulation are equal, which is the case here. But in general, the assumption to add the potential contributions P_p and P_i does not hold and the dual insulation approach in [4] should be considered.

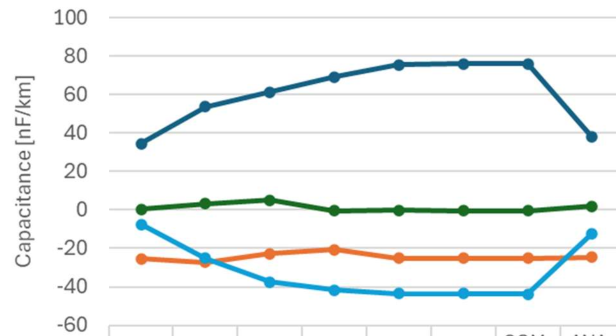

	0	5	10	20	50	75	COM-SOL	ANA-LYT
C11	34.537	53.513	61.201	69.057	75.26	75.763	75.809	37.939
C12	-25.46	-27.2	-22.79	-20.62	-25.08	-25.11	-25.07	-24.57
C13	0.247	3.272	5.064	-0.416	-0.262	-0.582	-0.557	1.978
C14	-7.53	-25.01	-37.42	-41.65	-43.43	-43.58	-43.69	-12.39

Fig. 14 Calculation of capacitance using MoM method as function of order N_p.

C. *Application, case 1*

This section shows the relevance of the proximity correction for Case 1. Fig. 15 shows how three different cable models are energized with a step voltage and Fig. 16 shows the simulated far end voltage of the energized phase (timestep 0.1 µs, and models fitted from 1 Hz-1 MHz). A cable parameter calculation routine is implemented in ATPDraw. This calculates series impedance and shunt admittance matrix with optionally proximity effect correction with MoM-SO for pipe-type cables. Vector fitting is also implemented for fitting of Y_c and H matrices and the ULM model [9] is called with required poles and residue file format. Fig. 16 compares the response of the ULM model with the standard JMarti model in ATP. The analytical formulas used in the ULM and JMarti models underestimate the damping somewhat, but velocity is correct.

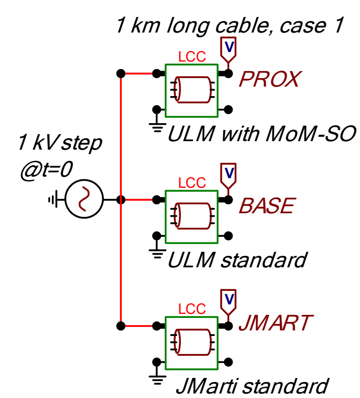

Fig. 15 Configuration for studying the effect of proximity correction for capacitance and series impedance.

The proximity effect on damping and velocity can be qualitatively analyzed based on the single-phase propagation factor $\gamma = \sqrt{z \cdot y} = \sqrt{(R \cdot k_R + j\omega L \cdot k_L) j\omega C \cdot k_C} = \alpha + j\omega / v$ where the proximity effect factors k_R and k_C>1 and k_L<1. With the real part of $z{\cdot}y$ dominating at high frequencies we can now approximate this as $\gamma \approx \alpha_0 \cdot k_R \sqrt{k_C / k_L} + j\omega / v_0 \cdot \sqrt{k_C k_L}$ where α_0 and β_0 are without proximity effect correction. Assuming that proximity affects L and C equally in opposite directions gives $k_L \cdot k_C \approx 1$. Ignoring proximity effect on capacitance (k_C=1) will thus increase the damping and velocity.

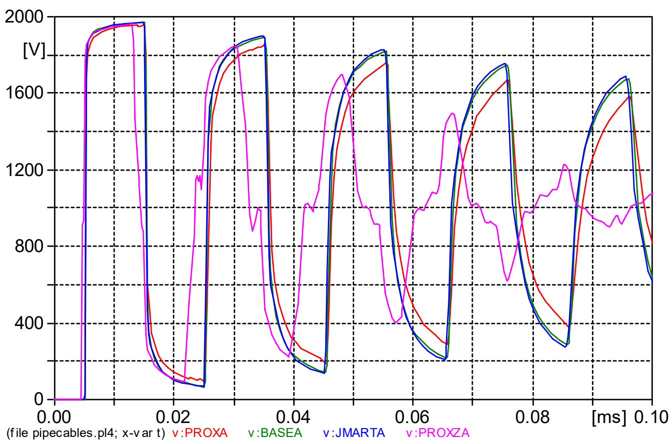

Fig. 16 Simulated far-end step response with and without proximity effect. BASEA and JMARTA voltages overlap. Red curve: with proximity effect. Magenta curve: proximity effect in impedance only.

V. Discussion

The paper compared calculation of cable impedance and capacitance in pipe-type cables. We use FEM calculation as a reference and compare this with analytical solutions and proximity effect correction with MoM approaches. The paper demonstrates severe deviations with analytical formulas and appropriate corrections with MoM methods. The calculation of incremental proximity effect contribution from MoM-SO allows a simple inclusion in classical cable parameter calculations without the need for the complications proposed in [4,10]. The proposed and implemented calculation process is typically faster than 1 s in cable cases where the order is limited to N_p=3 to 5. Tabl. III shows calculation times in the range 2.4-12.5 ms per frequency point for Case 1.

The brief presentation of the MoM-SO method and the elements of the Greens function in Sect. III showed that conductor ratios r_p/r_q are used in the expressions for the off-diagonal elements in G in (10). The required order of the method, N_p thus seems to depend on this ratio. Furthermore, the series expansion of (14)-(15) limits the order in practice for impedance calculations. In this work we have restricted the series expansion of Y_S up to order N_p=6. In [3] an order of N_p =4 was assumed to give sufficient accuracy. In this work we have seen that much higher order is required if the ratios of conductor radiuses are large. The calculation of capacitance requires only G and orders above 50 was required for Case 2.

Our study indicates that a maximum order in range of $N_P \approx 4 \cdot r_{\max} / r_{\min}$ is needed for high accuracy in capacitance C. For Case 2 in Fig. 4 this means an order of 4·162/5.5=118 would be required. Such high order will however result in ill-conditioned G-matrix as well as numerical problems for evaluation of the binomial coefficients (:). We have thus restricted expansion of the G-matrix in the final implementation to order N_p=40.

The authors in [4, 5] have proposed a method to calculate the capacitance in the case of mixed insulation. The conductor with insulation layer is equivalized with two boundary charges similar to tubular conductors in [3]. This method is not implemented in our work. The outer radius is used for the pipe -internal potential coefficients and added to the potential from the conductor P_i. This approach is not justified for the challenging Case 2.

VI. Conclusion

The paper compared calculation of impedance and capacitance in pipe-type cables. With FEM calculation as a reference, we have demonstrated severe deviations with analytical formulas and appropriate corrections with MoM methods.

The significance of the parameter correction is seen in the simulation in Fig. 16 where analytical formulas underestimate the resistance and give too low damping. With proximity effect corrections in series impedance only, the damping becomes too high and the velocity increases since the drop in inductance is not compensated by increase in capacitance.

For cases with large differences between conductor radiuses, a larger order number N_p is required. This is challenging for both calculation time and accuracy. Especially for impedance calculation in low conducting media this requires series expansion of complex Bessel functions for every order.

For dual insulation media with different dielectric permittivities, the expanded Greens function method proposed in [4, 5] should be considered.

VII. References

[1] A. Ametani, "A General Formulation of Impedance and Admittance of Cables," in *IEEE Transactions on Power Apparatus and Systems*, vol. PAS-99, no. 3, pp. 902-910, May 1980, doi: 10.1109/TPAS.1980.319718.

[2] U. R. Patel, B. Gustavsen and P. Triverio, "An Equivalent Surface Current Approach for the Computation of the Series Impedance of Power Cables with Inclusion of Skin and Proximity Effects," in *IEEE Transactions on Power Delivery*, vol. 28, no. 4, pp. 2474-2482, Oct. 2013, doi: 10.1109/TPWRD.2013.2267098.

[3] U. R. Patel, B. Gustavsen and P. Triverio, "Proximity-Aware Calculation of Cable Series Impedance for Systems of Solid and Hollow Conductors," *IEEE TRPWRD*, vol. 29, no. 5, pp. 2101-2109, 2014.

[4] Y. Tanaka, T. Noda, Y. Sekiba, E. Ito, K. Misawa, and T. Chida, “Development of a Computer Program for Calculating the Transmission-Line Constants of Cables Installed in a Tunnel Taking the Skin and Proximity Effects into Account”, IPST, 2017.

[5] Y. Tanaka and Y. Baba, "Development of a Method for Calculating the Capacitance of Cables Installed in a Rectangular Tunnel Taking Account of the Permittivity of the Outer Sheath," in *IEEE Transactions on Electromagnetic Compatibility*, vol. 65, no. 5, pp. 1422-1431, 2023.

[6] G. W. Brown, R. G. Rocamora, “Surge propagation in three-phase pipe-type cables, part I -Unsaturated pipe”, *IEEE Trans. Power App. Syst*., vol. PAS-95 , no. 1, part 1, pp. 89 – 95, 1976.

[7] B. Gustavsen, M. Høyer-Hansen, P. Triverio, and U. R. Patel. “Inclusion of Wire Twisting Effects in Cable Impedance Calculations”, *IEEE TRPWD*, Vol. 31, No. 6, pp 2520-2529, 2016.

[8] H. K. Høidalen, “Analysis of Pipe-type Cable Impedance Formulations at Low Frequencies”, *IEEE TRPWD*, Vol. 28, No. 4, pp. 2419-2427, 2013.

[9] F. O. S. Zanon, O. E. S. Leal, A. De Conti, “Implementation of the Universal Line Model in the Alternative Transients Program”, IPST 2021.

[10] U. R. Patel, Piero Triverio, “MoM-SO: A Complete Method for Computing the Impedance of Cable Systems Including Skin, Proximity, and Ground Return Effects”, *IEEE TRPWD*, Vol. 30, No. 5, pp. 2110-2018.